

Sensing Performances of Gaussian-shaped and Double-Side Unsymmetrical Metallic Nano-Gratings

Haiying Li and Xuesong Duan

School of sciences, Hebei University of technology, Tianjin, China
Email:lihaiying123@139.com

Abstract. A new type of sensing structure which is composed of a Gaussian-shaped and double-side unsymmetrical metallic nano-grating is presented. The reflectance spectra as functions of incident wavelengths in various refractive index conditions are analyzed by means of multiple multipole program (MMP) method. Our numerical simulation results show that the refractive index sensitivity (RIS) ~ 680 nm/RIU and the full-width at half-maximum (FWHM) ~ 3.5 nm can be obtained. The figure of merit (FOM) is over 190 RIU⁻¹. The resonant wavelength increases almost linearly with increasing of the refractive index of samples. These reflection properties not only give an insight into the physical mechanisms of the double-side unsymmetrical gratings, but also make this kind of nano-gratings more suitable to be used in the surface plasmon resonance (SPR) sensors.

1. Introduction

Free electron charges on the boundary of a metallic nanostructure can perform coherent fluctuations which are called surface plasmon resonance (SPR). For a certain frequency range of the exciting field, a complex resonant behavior can occur with strongly enhanced near-field and strong absorption of the electromagnetic waves [1-2]. SPR is highly sensitive to refractive index variation of the surrounding materials. These properties of SPR make the metallic nanostructures very popular for the application of sensing [3].

An approach with metallic nano-gratings incorporated into the SPR sensors has been proposed in recent years [4]. Use of metallic nano-gratings can enhance the refractive index sensitivity (RIS) by spectrum shifting of the peak resonant wavelength. Fortunately, focused ion beam milling (FIBM) technique provides a practical approach for fabrication of the nano-gratings [5-7]. The FIBM can realize one step direct fabrication of the nanostructures with finely controlled accuracy. However, a Gaussian profile-like shape instead of vertical sidewall of the structures in cross-section will be formed after the FIBM fabrication due to a Gaussian distribution of ion energy of the focused ion beam [8-9]. Sensing performances of metallic nano-gratings with single-side and double-side symmetrical Gaussian-shaped had been researched and reported by our group [10-11]. For obtaining higher RIS and larger FOM of the sensors, we put forth the investigation of sensing performances of the Gaussian-shaped and double-side unsymmetrical metallic nano-gratings in this paper. To our knowledge, it is first time to report the sensing performances of this type of gratings. Reflectance spectra of the sensing structure in various refractive index of the sample are calculated by multiple multipole program (MMP) method [12].



2. Modeling and Simulation Setup

There are three factors to determine the overall performance of the nano-gratings being used as an optical sensing chip. The first one is refractive index sensitivity(RIS), which is slope of the resonant wavelength over the refractive index. The second one is the full-width at half-maximum (FWHM) of the reflection curve, and The figure of merit (FOM), as the last one, is defined in reference[13] as follows:

$$\text{FOM} = \frac{\text{RIS}(\text{nm}/\text{RIU})}{\text{FWHM}(\text{nm})} \quad (1)$$

The overall performance of the optical sensors is affected by the FWHM. A wide FWHM makes it difficult to distinguish minor changes in the peak value. The depth of the resonance reflectance spectra can also affect sensitivity of the sensors.

A schematic diagram of the proposed metallic nano-grating is shown in Figure1. The model adopted in our work is a thin gold film with the unsymmetrical Gaussian-shaped grooves on both surfaces. The structure in a period is described mathematically as

$$z(x) = -H_2 \exp\left[-\left(\frac{x-x_1p}{w_2}\right)^2\right] - H_1 \exp\left[-\left(\frac{x-x_2p}{w_1}\right)^2\right], \text{ top} \quad (2)$$

$$z(x) = -(H_1 + t) + H_1 \exp\left[-\left(\frac{x-x_1p}{w_1}\right)^2\right] + H_2 \exp\left[-\left(\frac{x-x_2p}{w_2}\right)^2\right], \text{ bottom} \quad (3)$$

Here H_1 and H_2 represent the deeper groove depth and the shallower groove depth. W_1 and W_2 denote the deeper groove width and the shallower groove width respectively. P is the period of the metallic nano-gratings. The incomplete perforated film thickness $t > 0$. The sample is on top surface of the gold MNG with supported glass substrate.

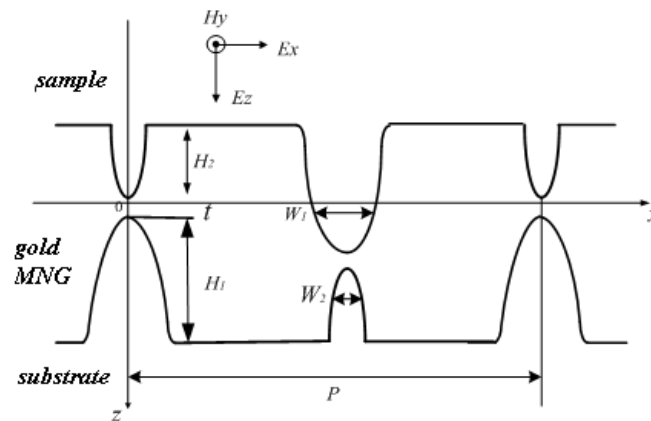


Figure1. Schematic diagram of MNG with Gaussian-shaped and double-side unsymmetrical grooves.

The reflection spectra were investigated using the MMP method[14]. The corresponding computational software is known as Max-1, which has first been proposed and developed in 1980 by Christian Hafner. MMP is a semi-analytic method for numerical field computations that has been applied to electromagnetic fields. Because of its close relations to analytic solutions, MMP is very useful and efficient when accurate and reliable solutions are desired.

3. Computational Results and Analyses

The optical constants of gold were taken from the experimental measurement [15]. Sample materials on the thin film have a refractive index ranging from 1.0 to 1.25. The substrate is SF10 glass with 1.72 refractive index. For TE polarization, surface oscillations do not exist because the electric field vector \vec{E} is parallel to the interface at which E is continuous across the boundary, and thus no surface charge is induced [16]. In our computational numerical simulation, a TM-polarized with a normal incidence

of light from the sample side is assumed, and the bandwidth of the incident light is set from 600 nm to 900 nm.

Influences of grating period P on reflectance and transmission spectra are investigated, which are shown in figure2(a) and figure2(b) respectively. Here the surface profile is defined by $t=15\text{nm}$, $H_1=40\text{nm}$, $H_2=20\text{nm}$, $W_1=W_2=50\text{nm}$, as P ranges from 600 nm to 800 nm. The sample is assumed to be air and its refractive index is 1.006. As can be seen from figure 2(b), when $P=600\text{nm}$, there is only one main peak at wavelength $\lambda = 638\text{nm}$. With the increasing of grating period the transmission peak becomes weaker, and its position moves to longer wavelength, which are 638nm, 729nm and 823nm respectively. From the dispersion relation of SPR, the resonant wavelength depends strongly on the structure period and the incident transverse wave vector. This can be expressed as equation (4):

$$k_{sp} = k_0 \sin \theta_0 + n \cdot \frac{2\pi}{p} \approx \left(\frac{\epsilon_m \cdot \epsilon_d}{\epsilon_m + \epsilon_d} \right)^{1/2} \cdot k_0 \quad (4)$$

Where k_{sp} and k_0 represent the wave vector of surface plasmons and wave vector in free space respectively, θ_0 is the incident angle, P is grating period. The SPR wavelengths can be calculated from equation (4), which are 626nm, 720nm and 816nm corresponding to period of 600, 700, 800nm respectively. With the comparison of the resonant positions, the narrow transmission peaks in Fig.2(b) can be identified as SPR wavelength, and the deviations may result from the incomplete perforated film thickness t . As expected, Fig. 2 shows that a peak in a transmission curve always corresponds to a minimum in the reflection curve at the same wavelength. SPR can form very deep and narrow reflection bands when grating period is 700nm. We find that the reflection curve can be deeper with a change of the groove width W_1 . In our following calculations, the optimized structure parameter is defined by $P=700\text{nm}$, $t=15\text{nm}$, $H_1=40\text{nm}$, $H_2=20\text{nm}$, $W_1=90\text{nm}$, $W_2=50\text{nm}$.

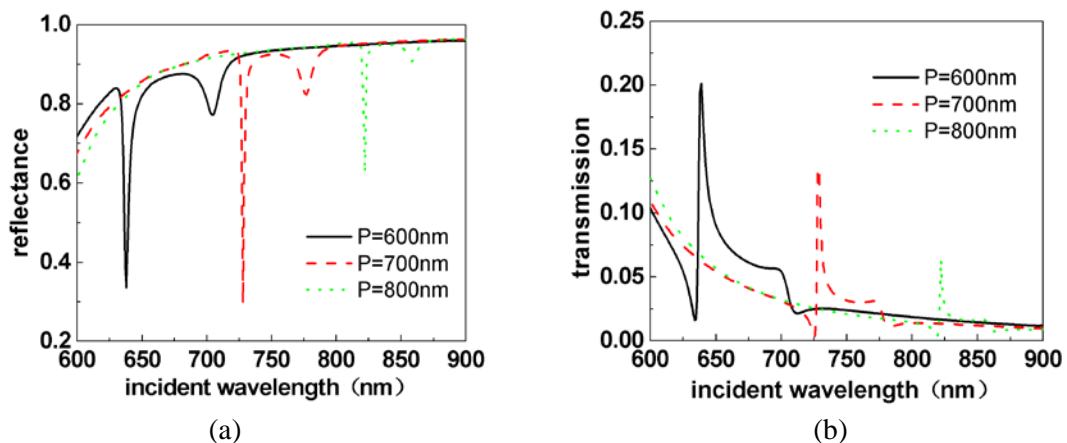


Figure2. Reflectance(a) and transmission(b) spectra as a function of incident wavelength for gold MNG with different periods as marked($t=15\text{nm}$, $H_1=40\text{nm}$, $H_2=20\text{nm}$, $W_1=W_2=50\text{nm}$).

The relationship between the reflection spectra and incident wavelength with 0.05 interval steps of refractive index of the sample was calculated, which can be seen in figure 3. With the increase of the sample refractive index, the resonant wavelength moves to longer wavelength. RIS of the structure can be obtained by the shift factor of the resonant wavelength. In order to compare the theoretical RIS and the calculated RIS, the relationship between resonant wavelength and sample refractive index is extracted from the data of figure 3, as shown in figure 4(a). The resonant wavelengths increase almost linearly with increasing of the sample refractive index. The theoretical results are obtained by equation(4). When the refractive index of sample increases from 1.0 to 1.25, the corresponding calculated resonant wavelength increases from 725.8nm to 896.8nm, and the theoretical resonant wavelength increases from 719.9nm to 896.5nm. So the theoretical RIS, i.e. the slope of the red line, is

~ 706.4 nm/RIU (RIU denotes refractive index unit). The calculated RIS, i.e. the slope of the black line, is ~ 684.0 nm/RIU, which is close to the theoretical results. FWHM of the reflection curve, which is extracted from the data of figure 3, is ~ 3.5 nm, as shown in figure 4 (b). The FOM is over 190RIU^{-1} while the refractive index value varies from 1.0 to 1.25.

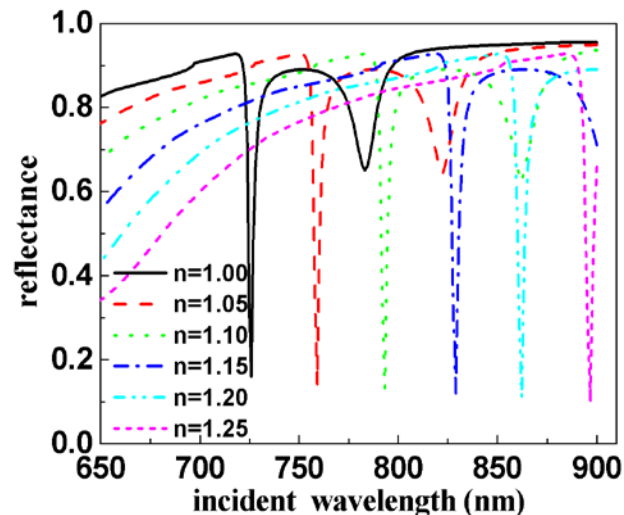


Figure3. Reflection spectra as a function of wavelength in various refractive index condition of sample ($P=700\text{nm}$, $t=15\text{nm}$, $H_1=40\text{nm}$, $H_2=20\text{nm}$, $W_1=90\text{nm}$, $W_2=50\text{nm}$).

Previously reported value of the RIS from literature is 490 nm/RIU for the one-side gaussian-shaped metallic nano-gratings[10], 420 nm/RIU for the double-side symmetrical metallic nano-gratings[11], 400 nm/RIU for the gold nanohole arrays [17], 328.5 nm/RIU for the gold nanoshells [18], and 150nm/RIU for LSPR sensors [19], respectively. The reported nanoparticles-based refractive index biosensors have a FOM value less than 10 due to a wide FWHM of the extinction spectrum [20]. Recently, a silver-coated side-polished fiber based SPR sensor was reported[21]. It has a higher RIS, but due to the wider FWHM, the FOM is less than 52RIU^{-1} . Sensing performances of the optimized Gaussian-shaped and double-Side unsymmetrical metallic nano-Gratings are superior to the performances of previously reported SPR sensors. Therefore, this type of the nano-grating based structure is more suitable to be used as a sensing chip because it can generate larger FOM.

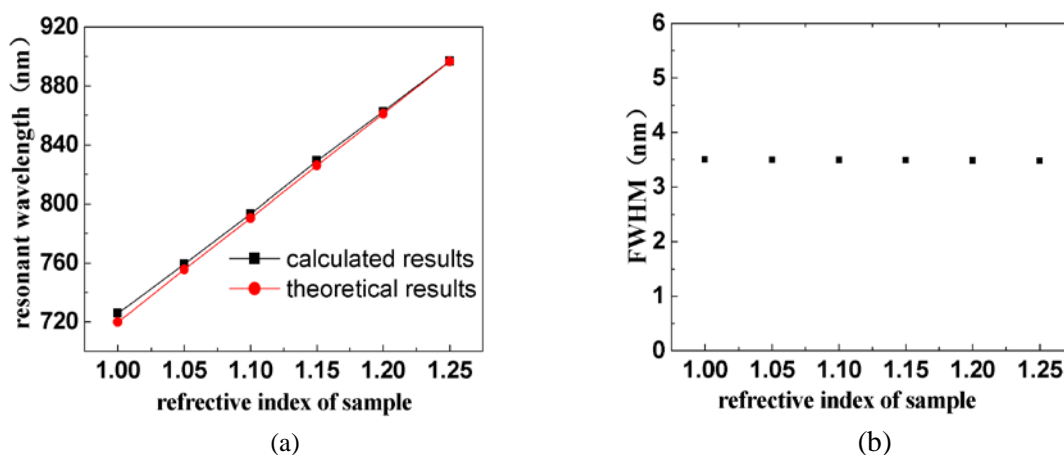


Figure4. (a) The relationship between resonant wavelength and refractive index of the sample; (b) The relationship between FWHM of reflective curve and sample refractive index which is extracted from the data of figure 3.

4. Conclusions

In summary, this paper puts forward a special type of metallic nano-Grating structure with Gaussian-shaped and double-Side unsymmetrical grooves. On the basis of the MMP method, reflection spectra as functions of wavelengths in various refractive index condition of the sample are theoretically analyzed by means of computational calculation and numerical simulation in nanofabrication point of view. For sensing application, two important factors, $RIS=684\text{nm}/RIU$ and $FOM=195RIU^{-1}$, can be achieved with the optimized structure. Therefore, it is reasonable to believe that these properties make this kind of nano-gratings more suitable to be used as a SPR-based sensing chip.

5. Acknowledgments

This work was supported by science and technology planning project of Hebei province (No.15210917) and Scientific Research Foundation of Hebei University of technology.

6. References

- [1] Heinz Raether, 1988, Surface Plasmons on smooth and rough surfaces and on gratings, Springer, pp91-116
- [2] Anatoly V. Zayats, Igor I. Smolyaninov, Alexei A. Maradudin, Nano-optics of surface plasmon polaritons, 2005, Physics Reports 408, pp131-314
- [3] J. Homola, S. S. Yee, G. Gauglitz, Surface plasmon resonance sensors: review, 1999, Sens. Actuators B 54, pp3-15
- [4] Kyung Hun Yoon, Michael L. Shuler, Sung June Kim, Design optimization of nano-grating surface plasmon resonance sensors, 2006, Optics Express 14, pp4842-4849
- [5] Yongqi Fu, Ngoi Kok Ann Bryan, Hybrid micro-diffractive-refractive optical element with continuous relief fabricated by focused ion beam for single-mode coupling, 2001, Applied Optics 40, pp5872-5876
- [6] Yongqi Fu, Ngoi Kok Ann Bryan, Ong Nan Shing, Experimental Study of 3D Microfabrication by Focused Ion Beam, 2000, Review of Scientific Instruments 71, pp1006-1008
- [7] Yongqi Fu, et al, Diffractive optical elements with continuous relief fabricated by focused ion beam for monomode fiber coupling, 2000, Optics Express 7, pp141-147
- [8] Yongqi Fu, Ngoi Kok Ann Bryan, Wei Zhou, A quasi-direct writing of diffractive structures using focused ion beam, 2004, Optics Express 12, pp1803-1809
- [9] Yongqi Fu, Ngoi Kok Ann Bryan, Spontaneously generated sinusoidal-like structures under focused ion beam bombardment, 2004, Optics Express 12, pp3707-3712
- [10] Haiying Li, Xiangang Luo, Chunlei Du, Xunan Chen and Yongqi Fu, Analysis of sensing performance of Gaussian-shaped metallic nano-gratings, 2008, Journal of Nanophotonics 2, p 023508
- [11] Haiying Li, Zhidong Zhang, Xiangang Luo, Xunan Chen, Yongqi Fu, Design of gaussian-shaped and double sides flanked metallic nano-grating surface plasma resonance biosensors, 2010, IEEE Symposium on Photonics and Optoelectronics
- [12] Ch. Hafner, The Multiple Multipole Program (MMP) and the Generalized Multipole Technique (GMT), 1999, In: Th. Wriedt (editor): Generalized Multipole Techniques for Electromagnetic and Light Scattering, Elsevier, Amsterdam
- [13] L. J. Sherry, S.-H. Chang, G. C. Schatz, R. P. Van Duyne, B. J. Wiley, and Y. Xia, Localized surface Plasmon Resonance Spectroscopy of single silver nanocubes, 2005, Nano Lett. 5, pp2034-2038
- [14] Esteban Moreno and Christian Hafner, Multiple multipole method with automatic multipole setting applied to the simulation of surface plasmons in metallic nanostructures, 2002, J. Opt. Soc. Am. A 19, pp101-111
- [15] P. B. Johnson and R. W. Christy, Optical constants of the noble metals, 1972, Phys. Rev. B 6, pp4370-4379
- [16] W.-C. Tan, T.W. Preist, and J.R. Sambles, Resonant tunneling of light through thin metal films via strongly localized surface plasmons, 2000, Phys. Rev. B 62, 11 pp 134-138

- [17] G. Brolo, R. Gordon, B. Leathem, and K. L. Kavanagh, Surface plasmon sensor based on the enhanced light transmission through arrays of nanoholes in gold films, 2004, *Langmuir* 20, pp 4813-4815
- [18] Y. G. Sun, and Y. N. Xia, Gold and silver nanoparticles: A class of chromophores with color tunable in the range from 400 to 750 nm, 2003, *Analyst* 128, pp 686-691
- [19] M. Duval Malinsky, K. Lance Kelly, G. C. Schatz, and R. P. Van Duyne, Chain length dependence and sensing capabilities of the localized surface plasmon resonance of silver nanoparticles chemically modified with Alkanethiol self-assembled monolayers, 2001, *J. Am. Chem. Soc.* 123, pp 1471-1482
- [20] N. Nath and A. Chilkoti, A colorimetric gold nanoparticle sensor to interrogate biomolecular interactions in real time on a surface, 2002, *Anal. Chem.* **74**, pp 504-509
- [21] Jing Zhao, et al. Surface plasmon resonance refractive sensor based on silver-coated side-polished fiber, 2016, *Sensors and Actuators B* 230, pp 206-211